ACS Sustainable Chemistry & Engineering

Research Article

pubs.acs.org/journal/ascecg

Demonstration of the $B_4C/NaIO_4$/PTFE Delay in the U.S. Army Hand-Held Signal

Anthony P. Shaw,* Jay C. Poret, Henry A. Grau, Jr., and Robert A. Gilbert, Jr.

Armament Research, Development and Engineering Center, U.S. Army RDECOM-ARDEC, Picatinny Arsenal, New Jersey 07806, United States

Supporting Information

ABSTRACT: A pyrotechnic time delay based on boron carbide has been demonstrated as a viable replacement for the perchlorate- and chromate-containing formulation currently used in U.S. Army hand-held signals. Tests involving fully assembled hand-held signal rockets were conducted to evaluate the characteristics of the $B_4C/NaIO_4$/PTFE delay system in an operational configuration. The delay times observed in such dynamic tests were substantially shorter than those expected from prior static testing, necessitating the use of very slow-burning compositions to achieve the desired 5−6 s dynamic delay time. The behavior of the system at extreme temperatures (−54 and +71 °C) was also evaluated, confirming its reliability and safety. Impact, friction, and electrostatic discharge tests have shown that the boron carbide-based delay is insensitive to unintended ignition. TGA/DSC analysis indicated an ignition temperature of 475 °C, well above the decomposition temperature of $NaIO_4$ and above the melting points of $NaIO_3$ and PTFE.

KEYWORDS: *Pyrotechnic delay, Boron carbide, Periodate, Hand-held signal, Sustainable chemistry*

INTRODUCTION

Pyrotechnic delays provide controlled intervals between energetic events.[1] They usually consist of consolidated pyrotechnic compositions that burn from end to end within small diameter metal channels.[2] Because of their simplicity and low cost, they are used extensively in fuzes for munitions such as grenades and in delay detonators for mining applications.[3−5] Pyrotechnic delays are also critical components of signaling devices issued to soldiers. For example, U.S. Army hand-held signals (HHS) contain a pyrotechnic delay to properly time the ignition and expulsion of illumination or smoke signaling payloads. This delay must burn for 5−6 s to allow the signal rocket to approach its apex before the payload is ignited and expelled.[6]

For many years, the U.S. Army has used pyrotechnics containing perchlorates, chromates, barium, and lead in HHS and other munitions. Pyrotechnic delay compositions have typically contained substantial amounts of barium chromate and potassium perchlorate as oxidizers, combined with powdered fuels such as tungsten, manganese, zirconium−nickel alloy, or amorphous boron.[7−10] On training ranges, residues leached from expended or dud munitions can potentially contaminate soil and groundwater. The regulation of hazardous substances[11−14] and concerns regarding perchlorate groundwater contamination[15] have motivated research on candidate replacement chemicals and formulations. Reformulation of the pyrotechnic compositions within HHS has been an objective of our research group for several years.[6,16−20]

A common delay composition, the tungsten delay, contains powdered tungsten as a fuel, barium chromate and potassium perchlorate as oxidizers, and diatomaceous earth as a diluent and flow agent.[7] A variant, lacking diatomaceous earth but containing a small amount of vinyl alcohol−acetate resin (VAAR) as a binder, is currently used in HHS.[21] Such compositions are suitable for use in a variety of hermetically sealed fuzes and delay elements, as they produce relatively little gas upon combustion. However, the HHS delay housing, which is not sealed, can also accommodate gas-producing compositions.

While numerous delay compositions free of chromates and perchlorates have been developed over the last 20 years,[4−6,20,22−29] few are able to burn slowly enough, without extinguishing, in the large pancake-shaped aluminum HHS delay housing. The short length of this housing necessitates an inverse burning rate of about 7−8.5 s/cm to provide the desired 5−6 s delay time. (The inverse burning rate is often the preferred metric for characterizing slow-burning delays.) From our previous static tests, only two experimental gas-producing systems appeared to be viable. The first, consisting of tungsten, antimony(III) oxide, potassium periodate, and a lubricant (usually calcium stearate), exhibited inverse burning rates of 2−15 s/cm.[6] The second, consisting of boron carbide, sodium periodate, and polytetrafluoroethylene (PTFE), provided an

Received: March 26, 2015
Revised: May 11, 2015
Published: May 20, 2015

DOI: 10.1021/acssuschemeng.5b00254
ACS Sustainable Chem. Eng. 2015, 3, 1558−1563

Report Documentation Page

Form Approved
OMB No. 0704-0188

1. REPORT DATE	2. REPORT TYPE	3. DATES COVERED
20 MAY 2015	**N/A**	**-**

4. TITLE AND SUBTITLE	5a. CONTRACT NUMBER
Demonstration of the B4C/NaIO4/PTFE Delay in the U.S. Army Hand-Held Signal	5b. GRANT NUMBER
	5c. PROGRAM ELEMENT NUMBER
6. AUTHOR(S)	5d. PROJECT NUMBER
Anthony P. Shaw, Jay C. Poret, Henry A. Grau, Jr., Robert A. Gilbert, Jr.	5e. TASK NUMBER
	5f. WORK UNIT NUMBER
7. PERFORMING ORGANIZATION NAME(S) AND ADDRESS(ES)	8. PERFORMING ORGANIZATION REPORT NUMBER
Armament Research, Development and Engineering Center, U.S. Army RDECOM-ARDEC, Picatinny Arsenal, New Jersey 07806, United States	
9. SPONSORING/MONITORING AGENCY NAME(S) AND ADDRESS(ES)	10. SPONSOR/MONITOR'S ACRONYM(S)
	11. SPONSOR/MONITOR'S REPORT NUMBER(S)

12. DISTRIBUTION/AVAILABILITY STATEMENT

Approved for public release, distribution unlimited

13. SUPPLEMENTARY NOTES

The original document contains color images.

14. ABSTRACT

A pyrotechnic time delay based on boron carbide has been demonstrated as a viable replacement for the perchlorate- and chromate-containing formulation currently used in U.S. Army hand-held signals. Tests involving fully assembled hand-held signal rockets were conducted to evaluate the characteristics of the B4C/NaIO4/PTFE delay system in an operational configuration. The delay times observed in such dynamic tests were substantially shorter than those expected from prior static testing, necessitating the use of very slowburning compositions to achieve the desired 5â6 s dynamic delay time. The behavior of the system at extreme temperatures (â54 and +71 Â°C) was also evaluated, confirming its reliability and safety. Impact, friction, and electrostatic discharge tests have shown that the boron carbide-based delay is insensitive to unintended ignition. TGA/DSC analysis indicated an ignition temperature of 475 Â°C, well above the decomposition temperature of NaIO4 and above the melting points of NaIO3 and PTFE.

15. SUBJECT TERMS

Pyrotechnic delay, Boron carbide, Periodate, Hand-held signal, Sustainable chemistry

16. SECURITY CLASSIFICATION OF:			17. LIMITATION OF ABSTRACT	18. NUMBER OF PAGES	19a. NAME OF RESPONSIBLE PERSON
a. REPORT	b. ABSTRACT	c. THIS PAGE			
unclassified	**unclassified**	**unclassified**	**UU**	**12**	

even broader range, 1−21 s/cm.[20] In both cases, the inverse burning rate may be precisely controlled by altering composition stoichiometry, component particle size, and consolidation force.

Later, it became evident that compositions containing mixtures of tungsten and periodate salts are susceptible to degradation in the presence of trace moisture.[29] The B_4C/$NaIO_4$/PTFE system, which does not present this complication, has been selected for further tests in fully assembled HHS. Herein, we describe the results of these prototype tests. The dynamic delay times obtained from firing fully assembled signal rockets are compared to static delay times obtained from igniting stand-alone delay elements. A selected delay composition was subjected to static and dynamic tests at extreme temperatures. The safety characteristics of a representative B_4C/$NaIO_4$/PTFE delay composition have been evaluated and are compared to those of tungsten-based delay compositions.

EXPERIMENTAL SECTION

Material Properties. Boron carbide powders (carbon rich, 19.0−21.7 wt % C) were obtained from Atlantic Equipment Engineers (AEE) and Alfa Aesar. The fine Alfa Aesar powder was blended in equal proportion with the coarser AEE material. Sodium periodate was obtained from Alfa Aesar and was separated into fractions using a 325 mesh (44 μm) screen; only the fine material was used. PTFE powder (type FL1650) was obtained from AGC Chemicals. For the fine sodium periodate fraction, a Malvern Morphologi G3S optical microscopy particle size analyzer was used to determine a number-based circle-equivalent diameter distribution, from which the volume-based distribution was calculated. For the boron carbide blend, a Microtrac S3500 laser diffraction particle size analyzer was used to determine the volume-based diameter distribution of an aqueous suspension. Particle size distributions are shown in Table 1. Material specifications for the tungsten delay and the tungsten-based HHS delay may be found in the Supporting Information.

Table 1. Particle Size Data for B_4C Delay Composition Components

component	$D[4,3]^a$	$D[v, 0.1]^b$	$D[v, 0.5]^b$	$D[v, 0.9]^b$
B_4C	11.25	2.72	9.72	20.46
$NaIO_4$	52.09	25.82	46.22	76.46
PTFE[c]		13.9	44.1	108.8

[a]Volume-based mean diameter in μm. [b]$D[v, x]$ is the diameter in μm that the fraction x of the volume distribution is below. [c]Manufacturer data.

Preparation of Compositions and Delay Elements. The B_4C delay compositions are three-component dry mixtures. For the experiments in Tables 2 and 3, small 12 g batches were prepared by sealing the components in a conductive container and mixing with a Scientific Industries Vortex Genie vibrating shaker. Each composition was mixed for 3 min followed by visual inspection for large aggregates (which, if present, were broken with a spatula) followed by another 3 min of mixing. For the experiments and tests in Tables 4 and 6, 35 g batches were prepared by a similar protocol except aggregates were broken by passing the mixtures through a 50 mesh (300 μm) screen.

The tungsten delay (MIL-T-23132A) is a dry mixture that was prepared on a 35 g scale by the screening protocol described above. The tungsten-based HHS delay (drawing 9251412) was prepared on a 40 g scale by mixing the dry components with an ethyl acetate solution of VAAR. Once most of the solvent had evaporated during mixing, the mixture was granulated through an 18 mesh (1.0 mm) screen and then dried in a 65 °C oven for several hours. These tungsten delay compositions were used for the tests in Table 6.

A Carver 3850 hydraulic press was used to load the B_4C delay compositions into aluminum HHS delay housings.[20] A dead load of 680 kg (376.6 MPa) or 1130 kg (627.6 MPa) was used for pressing, as indicated in the data tables. Black powder (class 7, 40−100 mesh, about 150−425 μm) was used for the input and output charges. To prepare each delay element, 50 mg of black powder was added and tamped, followed by the first half of the delay composition, followed by pressing. Then, the second half of the delay composition was added and tamped, followed by 50 mg of black powder, followed by pressing. The amount of delay composition was chosen so that the housings were substantially full after pressing. Delays loaded at 376.6 MPa contained 0.40 g of delay composition and those loaded at 627.6 MPa contained 0.42 g. Total column lengths, including the input and output charges, averaged 9.9 mm. The black powder input and output charges collectively occupied 2.7−2.8 mm of length in the cavity. The extent of consolidation of the delay columns (as %TMD) was calculated using 2.52, 3.86, and 2.3 g/cm^3 for the crystalline/maximum densities of B_4C, $NaIO_4$, and PTFE, respectively. The %TMD values may be found in the captions of Tables 2−4.

Test and Analysis Protocols. For static burning tests, the delay elements were conditioned in a temperature-controlled chamber overnight before testing. Each delay was mounted in a clamp and fired immediately after removal from the chamber, typically within 30 s. This involved placing 20−30 mg of loose black powder on top of the small hole of the delay element, which was then ignited with an electrically heated nichrome wire. Digital video recordings were used to measure the time between ignition and the first observed light of the output (the effective static delay time). Dynamic tests required conditioning fully assembled HHS overnight. The signal rockets were transported to the field in an insulated chamber and each was fired within 30 s of removal. The time between rocket launch and payload ejection (the effective dynamic delay time) was obtained by stopwatch. Tables 2−5 contain averaged delay times, and standard deviations are

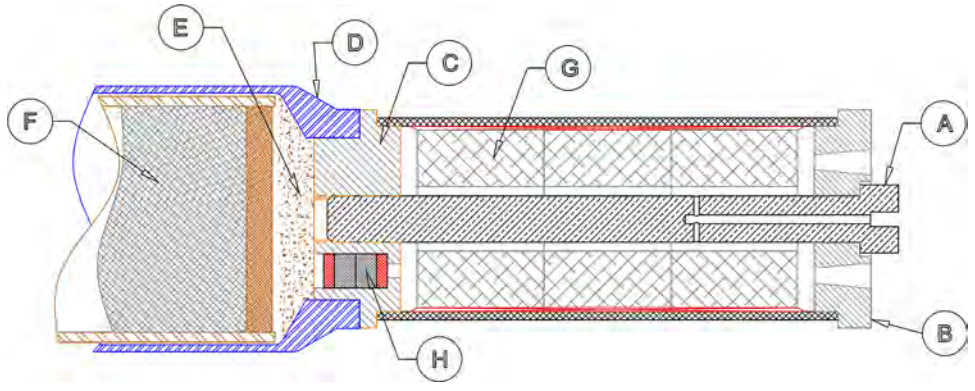

Figure 1. Partial cross section diagram of a hand-held signal showing the rocket motor, delay element, expelling charge, and pyrotechnic payload as they are assembled. The thin black powder input and output layers surrounding the delay column are shown in red.

DOI: 10.1021/acssuschemeng.5b00254
ACS Sustainable Chem. Eng. 2015, 3, 1558−1563

provided only as a rough approximation of the typical variation observed, for informational purposes. Precise comparison of these standard deviations is not possible due to the relatively small number of tests of each type.

Impact sensitivity tests were performed with a BAM drop hammer.[30] A Chilworth BAM friction apparatus was used for friction sensitivity testing.[31] A Safety Management Services ABL apparatus was used to test for electrostatic discharge (ESD) sensitivity.[32] Each composition was subjected to 10 impact and friction tests, and 20 electrostatic discharge tests. No ignition was observed. Thermal onset temperatures were determined with a PerkinElmer Diamond TGA/DSC. Alumina pans were used and the samples were heated at 5 °C/min under a 40 mL/min flow of nitrogen. The results of duplicate runs were averaged.

RESULTS AND DISCUSSION

Design and Configuration Considerations. Within HHS, the delay housing serves a structural role in addition to holding the delay column (Figure 1, Supporting Information). A bolt (**A**) holding the nozzle plate (**B**) at the end of the rocket assembly runs through the propellant combustion chamber, screwing into a threaded hole in the center of the delay housing (**C**). In turn, an interference fit fastens the delay housing to the signal rocket body (**D**) containing the expelling charge (**E**), pyrotechnic payload (**F**), and optionally a parachute. The black powder-based rocket motor, consisting of propellant pellets (**G**) encased in a cardboard tube, contains an axial core hole to accommodate the aforementioned bolt. The delay column (**H**) is contained within a cylindrical off-center cavity in the delay housing, in close proximity to the rocket motor. The delay housing, a 14.5 g machined aluminum part, has been described previously.[6,20] Unlike other delay housings, which are often elongated and tubular, the HHS delay housing is wider than it is long. In this configuration the delay column must burn slowly without extinguishing, despite substantial radial heat losses.

The HHS ignition train starts with a percussion primer. Once struck, this primer ignites a black powder initiating charge that ignites the rocket motor. Simultaneously, the delay element is ignited and burns for an interval (preferably 5−6 s) before it ignites the black powder expelling charge. The expelling charge ignites and ejects the pyrotechnic payload. Within the delay housing, thin black powder layers on both ends of the delay column ensure reliable ignition of the delay composition and provide an output flash sufficient for igniting the expelling charge. Importantly, even though the rocket motor burns for just 0.5 s, the delay column is directly exposed to pressure and heat within the combustion chamber during this time. Afterward, any gases generated by the burning delay composition vent, uninhibited, into this open chamber.

Static and Dynamic Delay Time Correlation. Stand-alone HHS delay elements are often tested statically, at ambient pressure and temperature, to ensure that each lot provides approximately the desired delay time. Dynamic delay times are then obtained during lot acceptance tests of fully assembled HHS. For delay elements containing the tungsten-based HHS delay composition, dynamic delay times are typically 0.5 s shorter than those measured in static tests. In this composition, which produces little gas upon combustion, the column burning front is propagated mainly through conductive heat transfer. The delay column remains substantially intact and the hot pressurized gases produced by the rocket motor cause only a minor decrease in measured delay time.

Burning $B_4C/NaIO_4$/PTFE delay compositions produce a substantial amount of gaseous combustion products. In these compositions, the column burning front appears to be propagated by conductive and convective heat transfer, with the extent of the latter depending on column porosity.[20] The extent to which radiative heat transfer participates in column burning is not known. Hot combustion gases carry away any condensed phase products leaving the housing mostly empty. The column burning front is continuously exposed and the burning rate is expected to be pressure-dependent, much like that of black powder.[33]

In static tests at ambient temperature, $B_4C/NaIO_4$/PTFE delay compositions loaded in HHS delay housings gave delay times ranging from 1 to 15 s.[20] However, it was not known which static delay time would correspond to the desired dynamic delay time of 5−6 s. It was also unknown how delay column porosity (or lack thereof) would affect dynamic performance. Five delay compositions with boron carbide contents ranging from 13 to 17 wt % were prepared. These were used to load hand-held signal delay elements at two different pressures. Moderate loading pressures yielded high consolidated densities due to the excellent lubricating properties of PTFE, which is present in all of the compositions at the 10 wt % level. Delay columns loaded at 376.6 MPa were consolidated to 93−96% of theoretical maximum density and therefore were slightly porous. Those loaded at 627.6 MPa were fully consolidated. The static and dynamic delay times, obtained at ambient temperature, are shown in Tables 2 and 3.

Table 2. Static and Dynamic Times for B_4C Delays Loaded at 376.6 MPa[a]

B_4C (wt %)	static time (s)	dynamic time (s)
17	6.62 (0.11)	3.66 (0.22)
16	7.47 (0.10)	4.00 (0.03)
15	8.52 (0.09)	4.52 (0.15)
14	10.30 (0.14)	5.49 (0.29)
13	11.90 (0.09)	6.61 (0.59)

[a]For compositions containing 13−17 wt % B_4C, 10 wt % PTFE, and $NaIO_4$ as the balance. Measured delay column densities ranged from 93 to 96% of the theoretical maxima. Five or six tests were used to determine each time and standard deviations are given in parentheses. All tests were conducted at ambient temperature (18−22 °C).

As expected for gas-producing compositions, and as discussed previously, the boron carbide-based delays tend to burn more slowly as column porosity decreases.[20] Thus, the delay columns in Table 3 generally burned more slowly than

Table 3. Static and Dynamic Times for B_4C Delays Loaded at 627.6 MPa[a]

B_4C (wt %)	static time (s)	dynamic time (s)
17	7.58 (0.10)	4.06 (0.41)
16	8.76 (0.44)	4.51 (0.29)
15	9.83 (0.25)	5.39 (0.87)
14		6.44 (0.53)
13		8.23 (0.67)

[a]For compositions containing 13−17 wt % B_4C, 10 wt % PTFE, and $NaIO_4$ as the balance. The delay columns were fully consolidated, with measured densities averaging 100% of the theoretical maxima. Delay columns containing 13 and 14 wt % B_4C did not ignite in static tests. Five or six tests were used to determine each time and standard deviations are given in parentheses. All tests were conducted at ambient temperature (18−22 °C).

DOI: 10.1021/acssuschemeng.5b00254
ACS Sustainable Chem. Eng. 2015, 3, 1558−1563

those in Table 2. Fully consolidated delay columns containing 13−14 wt % boron carbide failed in static tests but functioned when tested dynamically in signal rockets. In these delay columns, the burning front must be propagated by conductive (and perhaps radiative) heat transfer, since convection within the columns is not possible. The static failures are attributed to the low thermal conductivity of the compositions, boron carbide being the most thermally conductive component. Additionally, ignition of the delay compositions in static tests depends upon a relatively weak stimulus, a thin layer of black powder. The transient pressure and heat produced by the rocket motor during a dynamic test effectively provide a much stronger ignition impetus.

For any particular composition or loading pressure, the dynamic delay time was significantly shorter than the corresponding static time. A difference ranging from 3.0 to 5.3 s, corresponding to a relatively consistent 46% decrease, is caused by the pressure and heat within the rocket combustion chamber as the propellant burns. Remarkably, this substantial decrease in delay time occurs despite the rocket motor only burning for about 0.5 s. Two compositions, 14 wt % B_4C in Table 2 and 15 wt % B_4C in Table 3, gave dynamic delay times within the 5−6 s range desired for HHS. As it is preferable to test the delays statically without encountering failures, the lower loading pressure (376.6 MPa) was selected for further experiments. The data in Table 2 was used to construct a linear trend line, shown in Figure 2. Using this trend line, static delay times of 9.2−11.0 s should correspond to dynamic times of 5−6 s at ambient temperature.

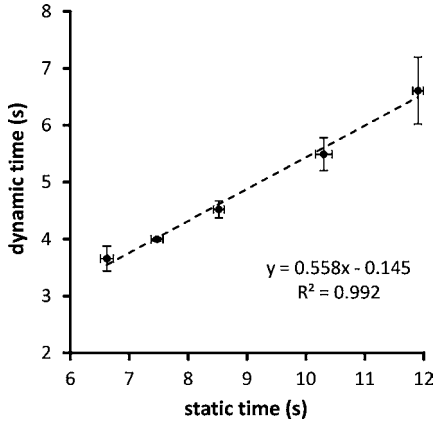

Figure 2. Plot, linear trend line, and equation for the data in Table 2. Error bars show two standard deviations.

Performance at Extreme Temperatures. HHS are tested at extreme temperatures, beyond what would be encountered in the field, to ensure reliability and safety. Cold testing at −54 °C is conducted to ensure the rockets will still function. Hot testing at 71 °C is performed mainly to ensure the rockets will not deflagrate upon functioning. As such, the dynamic delay times obtained from these tests are less critical, although the observed variations are recorded for informational purposes. A boron carbide-based delay composition with a static burning time of 10.2 s was selected for such tests (Table 4). As expected, cold temperature functioning gave lengthened delay times. Hot temperature functioning shortened the delay times to a lesser degree. The tungsten-based HHS delay, for which only dynamic delay times are available, exhibits the same trend but with less variation as a function of temperature (Table 5).

Table 4. Temperature Conditioning Tests of the B_4C Delay[a]

condition (temperature)	static time (s)	dynamic time (s)
hot (71 °C)	9.30 (0.12)	4.77 (0.29)
ambient (18−22 °C)	10.19 (0.15)	5.83 (0.42)
cold (−54 °C)	12.45 (0.79)	7.02 (0.39)

[a]For a composition containing approximately 13.8 wt % B_4C, 10 wt % PTFE, and $NaIO_4$ as the balance. Delays were loaded at 376.6 MPa. Measured delay column densities averaged 94% of the theoretical maximum. Ten tests were used to determine each time and standard deviations are given in parentheses.

Table 5. Dynamic Behavior of the Tungsten-based HHS Delay[a]

condition (temperature)	dynamic time (s)
hot (71 °C)	4.87 (0.22)
ambient (18−22 °C)	5.20 (0.15)
cold (−54 °C)	5.78 (0.17)

[a]Manufacturer data for a composition containing approximately 32 wt % W, 56.3 wt % $BaCrO_4$, 11.4 wt % $KClO_4$, and 0.3 wt % VAAR. Delays were loaded at approximately 500 MPa. Sixteen tests were used to determine each time and standard deviations are given in parentheses.

Most importantly, the $B_4C/NaIO_4$/PTFE system functions at −54 °C and does not deflagrate when tested at 71 °C, thereby ensuring reliability and safety at ordinary (less extreme) operating temperatures.

Sensitivity Tests and Thermal Analysis. Delay compositions are not generally considered to be hazardous when compared to other types of pyrotechnics.[34] However, extra caution must be reserved for any gas-producing composition, regardless of its burning rate. Accidental ignition of a gas-producing composition, especially a large quantity of unconsolidated powder typically encountered in a manufacturing environment, could lead to a violent deflagration. A representative $B_4C/NaIO_4$/PTFE delay composition was subjected to sensitivity tests (Table 6). A slow-burning tungsten delay composition and the tungsten-based HHS delay composition were tested to provide data for comparison. The data indicate that all three compositions are insensitive to impact, friction, and electrostatic discharge.

Thermal onset temperatures, as determined by TGA/DSC, show that the compositions in Table 6 ignite in the 450−500 °C range. The $B_4C/NaIO_4$/PTFE system ignites at about 475 °C, well above the decomposition temperature of $NaIO_4$.[35] At this temperature, both PTFE and $NaIO_3$ (the initial thermal decomposition product) are molten.[36,37] The presence of liquid phases at the ignition temperature distinguishes this system from the tungsten delay, which ignites in the solid state.[38,39]

Table 6. Sensitivity and Thermal Onset Data

composition	impact (J)	friction (N)	electrostatic discharge (mJ)	thermal onset (°C)
B_4C delay[a]	>31.9	>360	>250	475
tungsten delay[b]	>31.9	>360	>250	485
HHS delay[c]	>31.9	>360	>250	460

[a]17.5 wt % B_4C, 72.5 wt % $NaIO_4$, 10 wt % PTFE. [b]MIL-T-23132A containing 32 wt % W, 53 wt % $BaCrO_4$, 10 wt % $KClO_4$, 5 wt % diatomaceous earth. [c]32 wt % W, 56.3 wt % $BaCrO_4$, 11.4 wt % $KClO_4$, 0.3 wt % VAAR.

DOI: 10.1021/acssuschemeng.5b00254
ACS Sustainable Chem. Eng. 2015, 3, 1558−1563

Additional discussion pertaining to delay ignition mechanisms and the thermal analysis may be found in Supporting Information.

CONCLUSIONS

In summary, the $B_4C/NaIO_4$/PTFE delay has been demonstrated as an alternative to the currently specified formulation for HHS, which contains $KClO_4$ and $BaCrO_4$. The boron carbide-based delay compositions are gas-producing; this results in a significant difference between the observed static and dynamic delay times in the HHS configuration. A static delay time of 9.2−11.0 s is required to achieve the desired 5−6 s dynamic delay time at ambient temperature. The $B_4C/NaIO_4$/PTFE delay exhibits greater dynamic variability as a function of temperature than the tungsten-based delay in current use, but this should not adversely affect the functioning of HHS at expected operating temperatures. Importantly, the boron carbide-based delay compositions are insensitive to friction, impact, and electrostatic discharge. Thermal analysis indicates that liquid phases are present at the ignition temperature. The development and evaluation of highly tunable pyrotechnic delay systems continues to be an active area of research in our laboratories.

ASSOCIATED CONTENT

Supporting Information

Cross section diagrams of a hand-held signal (Figures S1 and S2); HHS delay housing and delay column configuration (Figure S3); specifications for the tungsten delay and the tungsten-based HHS delay (Tables S1 and S2); TGA/DSC plot for the boron carbide-based composition in Table 6 (Figure S4); additional discussion pertaining to thermal analysis. The Supporting Information is available free of charge on the ACS Publications website at DOI: 10.1021/acssuschemeng.5b00254.

AUTHOR INFORMATION

Corresponding Author

*A. P. Shaw. E-mail: anthony.p.shaw.civ@mail.mil.

Notes

The authors declare no competing financial interest.

This document has been approved by the U.S. Government for public release; distribution is unlimited.

ACKNOWLEDGMENTS

Karl D. Oyler and Jessica A. Vanatta are thanked for particle size measurements. Travis Fletcher and John Dixon are thanked for conducting the dynamic rocket tests. The U.S. Army is thanked for funding this work through the RDECOM Environmental Quality Technology Program. Table of contents photo credit, caption, and identifier: Master Sgt. Scott Wagers, U.S. Air Force; a U.S. Air Force security forces Airman fires an M127 parachute signal flare October 23, 2007, during Creek Defender at U.S. Army Garrison, Baumholder, Germany; defense imagery identification number 071023-F-EF201-098.

ABBREVIATIONS

ABL, Allegany Ballistics Laboratory
AEE, Atlantic Equipment Engineers
ARDEC, Armament Research, Development and Engineering Center
BAM, Bundesanstalt für Materialforschung und −prüfung
DSC, differential scanning calorimetry
ESD, electrostatic discharge
HHS, hand-held signal
PTFE, polytetrafluoroethylene
RDECOM, Research, Development and Engineering Command
TGA, thermogravimetric analysis
VAAR, vinyl alcohol−acetate resin
%TMD, consolidated density as a percentage of theoretical maximum density

REFERENCES

(1) Klapötke, T. M. *Chemistry of High-Energy Materials*, 2nd ed.; Walter de Gruyter: Berlin/Boston, 2012; section 2.5.1, pp 56−59.
(2) Wilson, M. A.; Hancox, R. J. Pyrotechnic delays and thermal sources. In *Pyrotechnic Chemistry: Pyrotechnic Reference Series No. 4*; Journal of Pyrotechnics, Inc.: Whitewater, CO, 2004; Chapter 8, pp 1−22.
(3) *Grenades and Pyrotechnic Signals*; Field Manual (FM 3-23.30); U.S. Army: Washington, DC, October 15, 2009.
(4) Tichapondwa, S. M.; Focke, W. W.; Del Fabbro, O.; Kelly, C. Calcium sulfate as a possible oxidant in "green" silicon-based pyrotechnic time delay compositions. *Propellants, Explos., Pyrotech.* **2014**, in press, DOI: 10.1002/prep.201400202.
(5) Swanepoel, D.; Del Fabbro, O.; Focke, W. W.; Conradie, C. Manganese as fuel in slow-burning pyrotechnic time delay compositions. *Propellants, Explos., Pyrotech.* **2010**, *35*, 105−113.
(6) Poret, J. C.; Shaw, A. P.; Csernica, C. M.; Oyler, K. D.; Estes, D. P. Development and performance of the $W/Sb_2O_3/KIO_4$/lubricant pyrotechnic delay in the US Army hand-held signal. *Propellants, Explos., Pyrotech.* **2013**, *38*, 35−40.
(7) *W/BaCrO$_4$/KClO$_4$/Diatomaceous Earth: Tungsten Delay Composition*, U.S. Military Specification MIL-T-23132A, June 16, 1972.
(8) *Mn/BaCrO$_4$/PbCrO$_4$: Manganese Delay Composition*, U.S. Military Specification MIL-M-21383A, October 22, 1976.
(9) *Zr-Ni/BaCrO$_4$/KClO$_4$: Composition, Delay*, U.S. Military Specification MIL-C-13739A, November 15, 1965.
(10) *B/BaCrO$_4$: Delay Composition, T-10*, U.S. Military Specification MIL-D-85306A, November 7, 1991.
(11) *Toxicological Profile for Perchlorates, Chapter 8: Regulations and Advisories*. Agency for Toxic Substances and Disease Registry, September, 2008; http://www.atsdr.cdc.gov/toxprofiles/tp162-c8.pdf (accessed March, 2015).
(12) *Toxicological Profile for Chromium, Chapter 8: Regulations, Advisories, and Guidelines*. Agency for Toxic Substances and Disease Registry, September, 2012; http://www.atsdr.cdc.gov/toxprofiles/tp7-c8.pdf (accessed March, 2015).
(13) *Toxicological Profile for Barium and Barium Compounds, Chapter 8: Regulations and Advisories*. Agency for Toxic Substances and Disease Registry, August, 2007; http://www.atsdr.cdc.gov/toxprofiles/tp24-c8.pdf (accessed March, 2015).
(14) *Toxicological Profile for Lead, Chapter 8: Regulations and Advisories*. Agency for Toxic Substances and Disease Registry, August, 2007; http://www.atsdr.cdc.gov/toxprofiles/tp13-c8.pdf (accessed March, 2015).
(15) Sellers, K.; Alsop, W.; Clough, S.; Hoyt, M.; Pugh, B.; Robb, J.; Weeks, K. *Perchlorate: Environmental Problems and Solutions*; CRC Press Taylor & Francis Group: Boca Raton, FL, 2007; Chapter 2, pp 7−42.
(16) Sabatini, J. J.; Moretti, J. D. High-nitrogen-based pyrotechnics: Perchlorate-free red- and green-light illuminants based on 5-aminotetrazole. *Chem.—Eur. J.* **2013**, *19*, 12839−12845.
(17) Sabatini, J. J.; Raab, J. M.; Hann, R. K.; Freeman, C. T. Brighter- and longer-burning barium-free illuminants for military and civilian pyrotechnics. *Z. Anorg. Allg. Chem.* **2013**, *639*, 25−30.
(18) Moretti, J. D.; Sabatini, J. J.; Shaw, A. P.; Chen, G.; Gilbert, R. A.; Oyler, K. D. Prototype scale development of an environmentally

DOI: 10.1021/acssuschemeng.5b00254
ACS Sustainable Chem. Eng. 2015, 3, 1558−1563

benign yellow smoke hand-held signal formulation based on solvent yellow 33. *ACS Sustainable Chem. Eng.* **2013**, *1*, 673−678.
(19) Moretti, J. D.; Sabatini, J. J.; Shaw, A. P.; Gilbert, R. Promising properties and system demonstration of an environmentally benign yellow smoke formulation for hand-held signals. *ACS Sustainable Chem. Eng.* **2014**, *2*, 1325−1330.
(20) Poret, J. C.; Shaw, A. P.; Csernica, C. M.; Oyler, K. D.; Vanatta, J. A.; Chen, G. Versatile boron carbide-based energetic time delay compositions. *ACS Sustainable Chem. Eng.* **2013**, *1*, 1333−1338.
(21) *W/BaCrO$_4$/KClO$_4$/VAAR: Delay Assembly*; drawing 9251412; U.S. Army Armament Research and Development Center: Picatinny Arsenal, NJ, July 1, 1971.
(22) Rugunanan, R. A.; Brown, M. E. Combustion of binary and ternary silicon/oxidant pyrotechnic systems, Part IV: Kinetic aspects. *Combust. Sci. Technol.* **1993**, *95*, 117−138.
(23) Brammer, A. J.; Charsley, E. L.; Griffiths, T. T.; Rooney, J. J.; Warrington, S. B. A study of the pyrotechnic performance of the silicon-bismuth oxide system. *Proceedings of the 22nd International Pyrotechnics Seminar*, Fort Collins, CO, July 15−19, 1996; pp 447−460.
(24) Ricco, I. M. M.; Focke, W. W.; Conradie, C. Alternative oxidants for silicon fuel in time-delay compositions. *Combust. Sci. Technol.* **2004**, *176*, 1565−1575.
(25) Kalombo, L.; Del Fabbro, O.; Conradie, C.; Focke, W. W. Sb_6O_{13} and Bi_2O_3 as oxidants for Si in pyrotechnic time delay compositions. *Propellants, Explos., Pyrotech.* **2007**, *32*, 454−460.
(26) Rose, J. E.; Michay, M.; Puszynski, J. Non-toxic pyrotechnic delay compositions. U.S. Patent 7,883,593 B1, February 8, 2011.
(27) Miklaszewski, E. J.; Poret, J. C.; Shaw, A. P.; Son, S. F.; Groven, L. J. Ti/C-3Ni/Al as a replacement time delay composition. *Propellants, Explos., Pyrotech.* **2014**, *39*, 138−147.
(28) Miklaszewski, E. J.; Shaw, A. P.; Poret, J. C.; Son, S. F.; Groven, L. J. Performance and aging of Mn/MnO_2 as an environmentally friendly energetic time delay composition. *ACS Sustainable Chem. Eng.* **2014**, *2*, 1312−1317.
(29) Poret, J. C.; Shaw, A. P.; Miklaszewski, E. J.; Groven, L. J.; Csernica, C. M.; Chen, G. Environmentally benign energetic time delay compositions: Alternatives for the U.S. Army hand-held signal. *Proceedings of the 40th International Pyrotechnics Seminar*; Colorado Springs, CO, July 13−18, 2014; pp 305−314. Available via Defense Technical Information Center (DTIC), accession number ADA603699.
(30) Standardization agreement (STANAG) 4489: *Explosives, Impact Sensitivity Tests*; 1st ed.; NATO Military Agency for Standardization: Brussels, Belgium, September 17, 1999.
(31) Standardization agreement (STANAG) 4487: *Explosives, Friction Sensitivity Tests*; 1st ed.; NATO Standardization Agency: Brussels, Belgium, August 22, 2002.
(32) Standardization agreement (STANAG) 4490: *Explosives, Electrostatic Discharge Sensitivity Tests*; 1st ed.; NATO Military Agency for Standardization: Brussels, Belgium, February 19, 2001.
(33) Sasse, R. A. *A Comprehensive Review of Black Powder*; accession number ADA150455; Defense Technical Information Center (DTIC): Fort Belvoir, VA, 1985; pp 1−41.
(34) McIntyre, F. L. *A Compilation of Hazard and Test Data for Pyrotechnic Compositions*; accession number ADA096248; Defense Technical Information Center (DTIC): Fort Belvoir, VA, 1980; pp 1−382.
(35) Muraleedharan, K.; Kannan, M. P. Thermal decomposition kinetics of sodium metaperiodate. *React. Kinet. Catal. Lett.* **1989**, *39*, 339−344.
(36) Khanna, Y. P. The melting temperature of polytetrafluoroethylene. *J. Mater. Sci. Lett.* **1988**, *7*, 817−818.
(37) Stern, K. H. *High Temperature Properties and Thermal Decomposition of Inorganic Salts with Oxyanions*; CRC Press: Boca Raton, FL, 2001; Chapters 7 and 9.
(38) Zimmer-Galler, R. *The Combustion of Tungsten and Manganese Delay Systems*; accession number AD0879499; Defense Technical Information Center (DTIC): Fort Belvoir, VA, 1970; pp 1−33.
(39) Shachar, E.; Gany, A. Investigation of slow-propagation tungsten delay mixtures. *Propellants, Explos., Pyrotech.* **1997**, *22*, 207−211.

DOI: 10.1021/acssuschemeng.5b00254
ACS Sustainable Chem. Eng. 2015, 3, 1558−1563

Supporting Information

Demonstration of the $B_4C/NaIO_4$/PTFE Delay in the U.S. Army Hand-Held Signal

Anthony P. Shaw,* Jay C. Poret, Henry A. Grau, Jr., Robert A. Gilbert, Jr.

Armament Research, Development and Engineering Center, U.S. Army RDECOM-ARDEC, Picatinny Arsenal, NJ 07806, USA

*e-mail: anthony.p.shaw.civ@mail.mil

Contents:

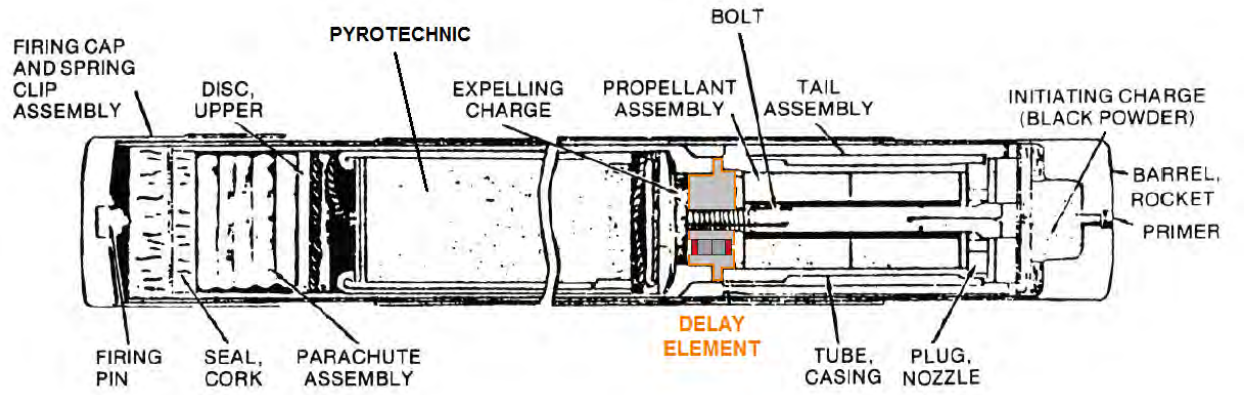

Figure S1. Cross section diagram of a hand-held signal. The delay element is outlined in orange. The thin black powder input and output layers surrounding the delay column are shown in red.

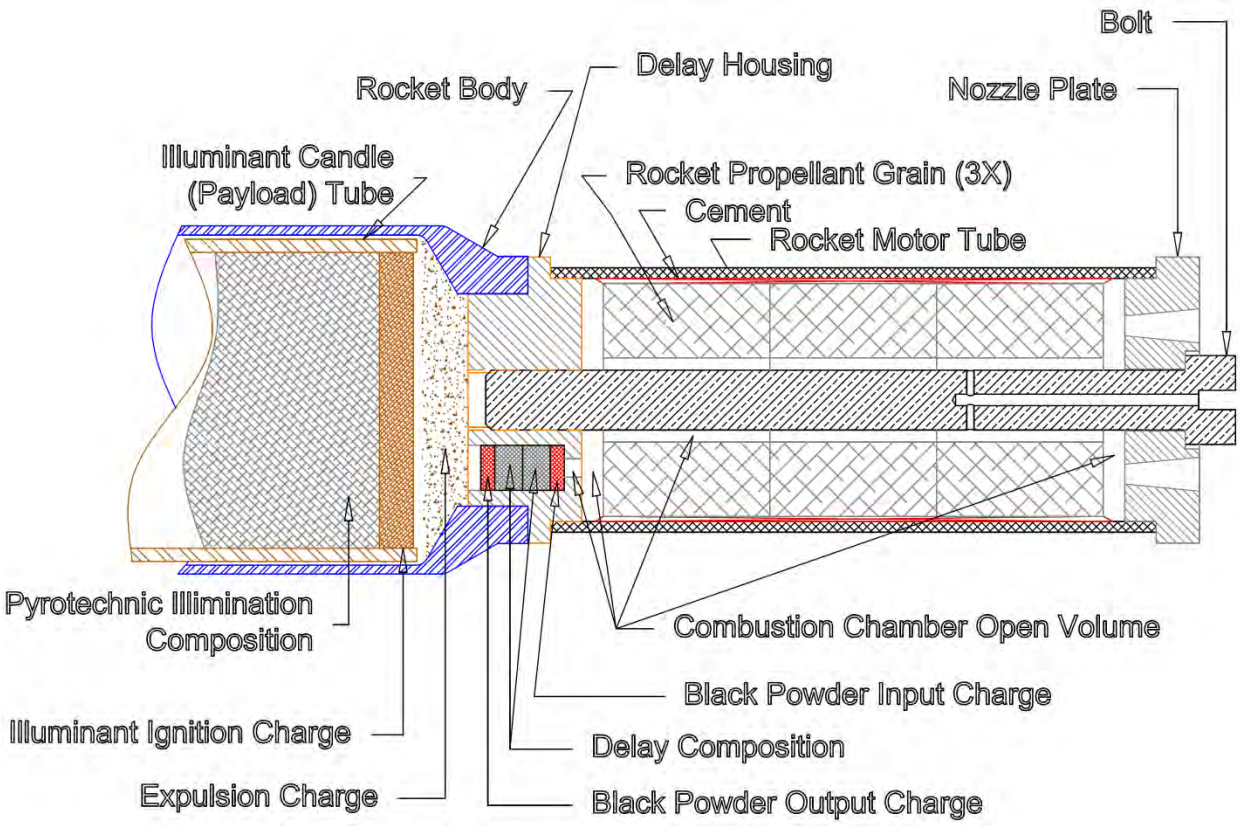

Figure S2. Partial cross section diagram of a hand-held signal. The delay element is outlined in orange, with the 1.9 mm diameter opening on the right facing the rocket motor and the 4.8 mm diameter opening on the left facing the expelling charge.

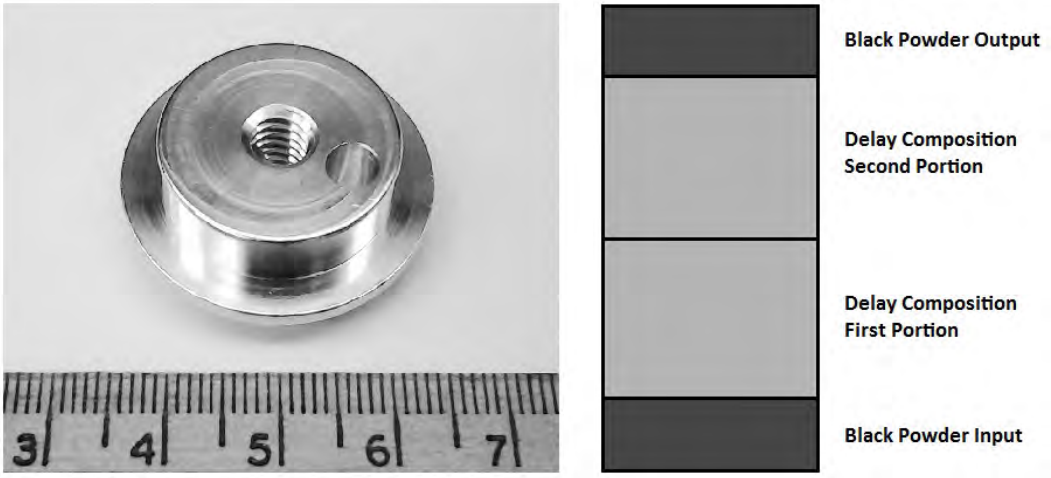

Figure S3. HHS delay housing and delay column configuration. The output side of the housing is shown. The delay column and black powder layers occupy the off-center 4.8 mm diameter cavity which is 10.2 mm long. With the black powder charges occupying 2.7-2.8 mm of length, just 7.4-7.5 mm remains for delay composition.

Table S1. Specifications for the Tungsten Delay. [a)]

Component	Amount (wt%) [b)]	Specification	Type, Grade, Class
tungsten	32	AS-2686	type 2
barium chromate	53	MIL-B-550	grade A
potassium perchlorate	10	MIL-P-217	grade A
diatomaceous earth	5	MIL-D-20550	grade B

a) MIL-T-23132A. b) This particular composition was used for the tests in Table 6.

Table S2. Specifications for the Tungsten-Based HHS Delay. [a)]

Component	Amount (wt%)	Specification	Type, Grade, Class
tungsten	32	MIL-T-48140	type 1
barium chromate	56.3	MIL-B-550	grade C
potassium perchlorate	11.4	MIL-P-217	grade A, class 4
VAAR [b)]	0.3 [c)]	MIL-V-50433	

a) Drawing 9251412. b) Vinyl alcohol-acetate resin. c) Refers to solids.

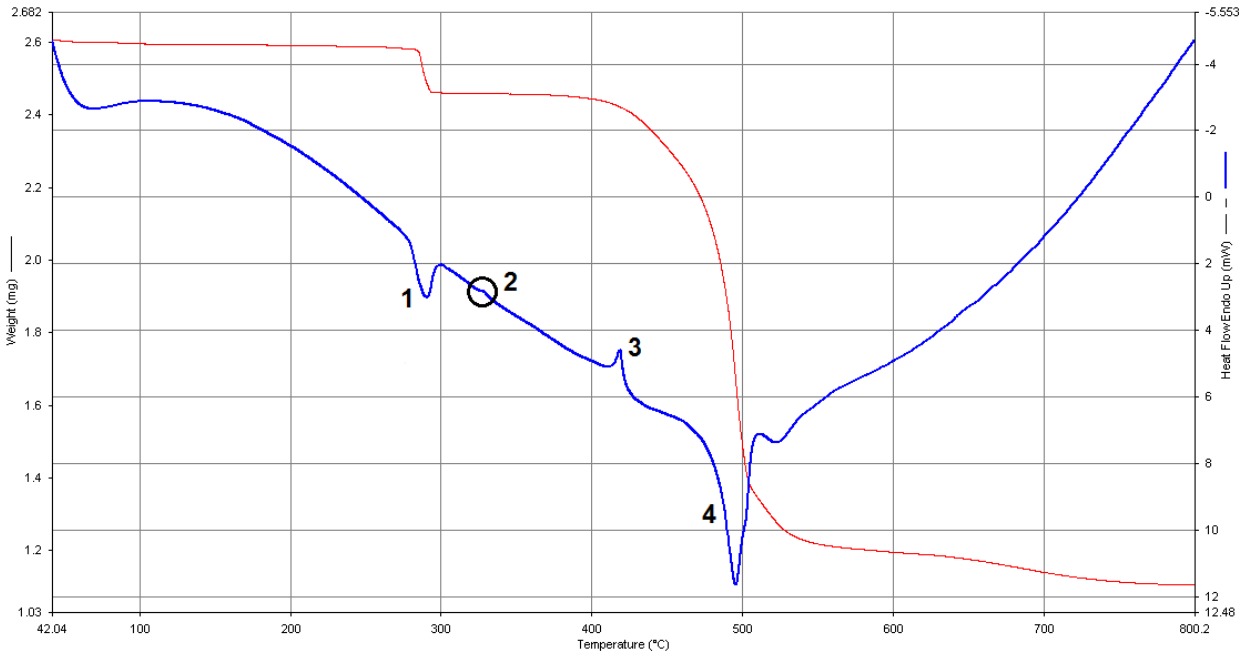

Figure S4. TGA/DSC plot for the boron carbide-based delay composition in Table 6. The sample was heated at 5 °C/min under a 40 mL/min flow of nitrogen. Heat flow (blue line) and sample weight (red line) were recorded as a function of temperature. Numbers mark the events leading to thermal ignition. Initial decomposition of $NaIO_4$ (exothermic, **1**); melting of PTFE (endothermic, **2**); melting of $NaIO_3$ (endothermic, **3**); thermal onset and ignition (exothermic, **4**).

Additional Discussion Pertaining to Thermal Analysis:

Ignition of the tungsten delay has been shown to depend on $KClO_4$. Binary W/$BaCrO_4$ mixtures do not ignite [1,2]. In this system, melting of the oxidizer is not observed prior to ignition. Potassium perchlorate is believed to melt at approximately 580 °C accompanied by rapid decomposition [3], yet tungsten delay compositions often ignite between 450-500 °C. The slow decomposition of solid $KClO_4$ in this temperature range provides enough free oxygen to trigger ignition. The presence of organic materials, such as VAAR in the variant used for HHS, tends to lower the ignition temperature, as shown in Table 6.

In contrast to the thermal decomposition of $KClO_4$, which leads to KCl and O_2, the complete thermal decomposition of $NaIO_4$ proceeds in very distinct steps. Without melting, $NaIO_4$ decomposes exothermically between 260-315 °C to give $NaIO_3$ and O_2 (eq 1) [4]. Then, $NaIO_3$ melts at 422 °C (eq 2) [3]. Molten $NaIO_3$ undergoes endothermic decomposition rapidly above 460 °C giving NaI and O_2 (eq 3), although formation of Na_2O, I_2, and O_2 is also possible (eq 4) [3]. The related potassium salt (KIO_4) follows a similar step-wise pathway but the KIO_3 intermediate begins to decompose before melting [3,5,6]. Purple smoke emitted by delay compositions containing periodate salts is attributed to I_2 formation (as shown in eq 4) [7-9].

$$2\ NaIO_{4\,(s)} \rightarrow 2\ NaIO_{3\,(s)} + O_{2\,(g)} \qquad \text{(eq 1)}$$

$$NaIO_{3\,(s)} \rightarrow NaIO_{3\,(l)} \qquad \text{(eq 2)}$$

$$2\ NaIO_{3\,(l)} \rightarrow 2\ NaI_{(s)} + 3\ O_{2\,(g)} \qquad \text{(eq 3)}$$

$$4\ NaIO_{3\,(l)} \rightarrow 2\ Na_2O_{(s)} + 2\ I_{2\,(g)} + 5\ O_{2\,(g)} \qquad \text{(eq 4)}$$

Thermal onset in the $B_4C/NaIO_4$/PTFE system occurs at about 475 °C, only *after* the $NaIO_3$ formed in eq 1 is molten and begins to decompose (Figure S4). At this point the PTFE, with a melting point of 327 °C, is also molten [10]. Ignition appears to depend on $NaIO_3$ decomposition, since binary B_4C/PTFE compositions do not ignite [8] and PTFE does not undergo appreciable thermal decomposition below 500 °C [11,12].

References:

[1] Zimmer-Galler, R. *The Combustion of Tungsten and Manganese Delay Systems*; accession number AD0879499; Defense Technical Information Center (DTIC): Fort Belvoir, VA, 1970; pp 1-33.

[2] Shachar, E.; Gany, A. Investigation of Slow-Propagation Tungsten Delay Mixtures. *Propellants, Explos., Pyrotech.* **1997**, *22*, 207-211.

[3] Stern, K. H. *High Temperature Properties and Thermal Decomposition of Inorganic Salts with Oxyanions*; CRC Press: Boca Raton, FL, 2001; Chapters 7 and 9.

[4] Muraleedharan, K.; Kannan, M. P. Thermal Decomposition Kinetics of Sodium Metaperiodate. *React. Kinet. Catal. Lett.* **1989**, *39*, 339-344.

[5] Muraleedharan, K.; Kannan, M. P.; Gangadevi, T. Effect of Metal Oxide Additives on the Thermal Decomposition Kinetics of Potassium Metaperiodate. *J. Therm. Anal. Calorim.* **2010**, *100*, 177-181.

[6] Muraleedharan, K.; Kannan, M. P.; Gangadevi, T. Thermal Decomposition Kinetics of Potassium Iodate. *J. Therm. Anal. Calorim.* **2011**, *103*, 943-955.

[7] Poret, J. C.; Shaw, A. P.; Csernica, C. M.; Oyler, K. D.; Estes, D. P. Development and Performance of the $W/Sb_2O_3/KIO_4$/Lubricant Pyrotechnic Delay in the US Army Hand-Held Signal. *Propellants, Explos., Pyrotech.* **2013**, *38*, 35-40.

[8] Poret, J. C.; Shaw, A. P.; Csernica, C. M.; Oyler, K. D.; Vanatta, J. A.; Chen, G. Versatile Boron Carbide-Based Energetic Time Delay Compositions. *ACS Sustainable Chem. Eng.* **2013**, *1*, 1333-1338.

[9] Poret, J. C.; Shaw, A. P.; Miklaszewski, E. J.; Groven, L. J.; Csernica, C. M.; Chen, G. Environmentally Benign Energetic Time Delay Compositions: Alternatives for the U.S. Army Hand-Held Signal. *Proceedings of the 40th International Pyrotechnics Seminar*; Colorado Springs, CO, USA, July 13-18, 2014; pp 305-314. Available via Defense Technical Information Center (DTIC), accession number ADA603699.

[10] The melting point of as-polymerized PTFE is greater than that of annealed or recrystallized samples: Khanna, Y. P. The Melting Temperature of Polytetrafluoroethylene. *J. Mater. Sci. Lett.* **1988**, *7*, 817-818.

[11] Beyler, C. L.; Hirschler, M. M. Thermal Decomposition of Polymers. In *SFPE Handbook of Fire Protection Engineering*, 3rd ed; DiNenno, P. J., Ed; National Fire Protection Association: Quincy, MA, 2002; Section 1, Chapter 7, pp 110-131.

[12] Koch, E.-C. *Metal-Fluorocarbon Based Energetic Materials*; Wiley-VCH Verlag & Co.: Weinheim, Germany, 2012; pp 20-22.